CRYSTAL GROWTH & DESIGN

pubs.acs.org/crystal

Article

Morphology Evolution of a h-BN Film Grown by Halide Vapor Phase Epitaxy at Different Growth Temperatures

Ting Liu,[⊥] Zhijie Shen,[⊥] Minghao Chen, Qian Zhang, Maosong Sun, Chunlei Fang, Yong Lu, Hai Hu, Shuxin Tan,* and Jicai Zhang*

Cite This: *Cryst. Growth Des.* 2024, 24, 810−816

Read Online

ACCESS | Metrics & More | Article Recommendations | Supporting Information

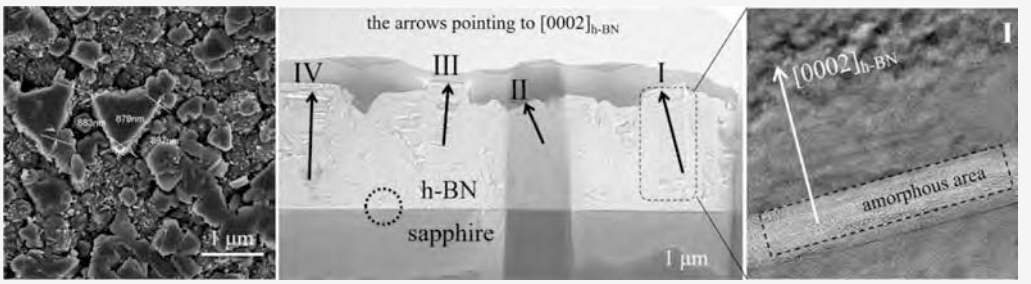

ABSTRACT: Micron-thick BN films are prepared on 2 in. *c*-plane sapphire substrates using low-pressure halide vapor phase epitaxy, with BCl_3 and NH_3 being utilized as the respective sources of boron and nitrogen. The morphology and crystal quality of BN films grown at temperatures ranging from 1050 to 1650 °C are systematically investigated. X-ray diffraction analysis demonstrates that the synthesized films are primarily oriented along the [0002] direction of hexagonal boron nitride (h-BN), although a small amount of turbostratic BN is also observed. Scanning electron microscopy measurements reveal a typical layered stacking morphology in the cross section of h-BN films. As the growth temperature rises, h-BN has a tendency to transition from a 3D to a 2D growth mode, as seen by the coalescence of h-BN nanograins to form smooth micron-scale triangular grains. Transmission electron microscopy characterization shows that these triangular grains are well-crystallized [0002]-oriented h-BN phases, with minor variations in crystallographic orientations among individual grains. While these micron-scale triangular grains have not yet coalesced into larger grains, further refinement of the growth conditions holds the potential to induce their coalescence, resulting in the formation of continuous thick h-BN films with high crystal quality.

INTRODUCTION

Hexagonal boron nitride (h-BN) is a III−V nitride, characterized by a wide band gap of 6.0 eV,[1] making it a highly promising candidate for use in deep ultraviolet optoelectronics and high-power electronics.[2] h-BN exhibits excellent mechanical properties, a low dielectric constant, and remarkable high-temperature stability.[3] It has a layered structure similar to graphite and is held together by van der Waals (vdW) forces.[4] Moreover, due to the small lattice mismatch (2%) between h-BN and graphene, atomically smooth surfaces, and the absence of dangling bonds, h-BN serves as a suitable substrate material for graphene-based devices.[5] Furthermore, there has been significant interest in neutron detectors,[6] spin characteristics,[7] and flexural electrical effects utilizing large-sized h-BN single crystals.[8] However, the size of h-BN bulk single crystals synthesized by nickel−molybdenum solvents at atmospheric pressure or prepared by high-temperature and high-pressure liquid-phase reactions is typically constrained to a few hundred microns.[9] Consequently, the fabrication of single-crystalline h-BN thick films (≥1 μm) on large-sized substrates (≥2 in.) like sapphire, silicon, and silicon carbide stands as a viable alternative to bulk crystalline materials.[10] Nevertheless, the synthesis of large, thick, single-crystal vdW materials remains a substantial challenge due to the absence of out-of-plane chemical bonds, which weakens the epitaxial relationship between adjacent layers.[11]

Metal−organic chemical vapor deposition,[12] molecular beam epitaxy,[13] ion beam sputtering deposition,[14] and submicron-spacing vapor deposition[15] have been confirmed to be capable of growing high-quality few-layer h-BN films, while their limited growth rate makes them unsuitable for the rapid and cost-effective preparation of large-size single-crystal h-BN thick films (≥1 μm). Previous research has shown that halide vapor phase epitaxy (HVPE) is a viable approach for rapidly

Received: October 19, 2023
Revised: December 22, 2023
Accepted: December 26, 2023
Published: January 5, 2024

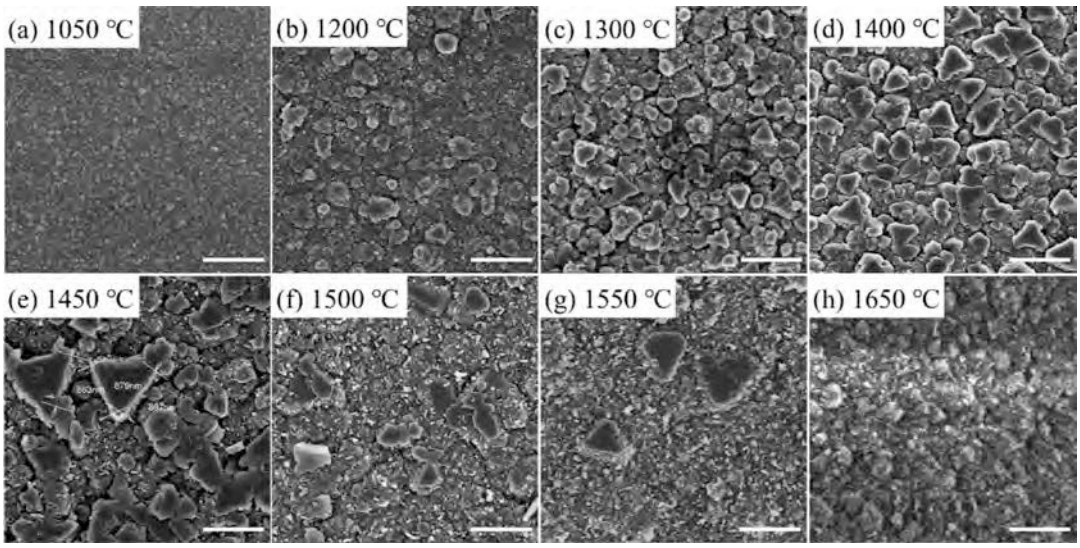

Figure 1. Surface SEM images of h-BN films grown at different temperatures. (a) 1050 °C. (b) 1200 °C. (c) 1300 °C. (d) 1400 °C. (e) 1450 °C. (f) 1500 °C. (g) 1550 °C. (h) 1650 °C. The scale bar is 1 μm.

fabricating thick films of large-size single-crystal III−V nitride semiconductors like GaN and AlN.[16] For the growth of h-BN by HVPE, boron trichloride (BCl_3) and ammonia (NH_3) are employed as source gases, taking into consideration the current commercial utilization of this combination for the rapid growth of pyrolytic BN.[17] To achieve the epitaxial growth of single-phase h-BN, it is essential to effectively address these three key challenges: parasitic reactions among the source gases, the exceedingly high growth temperature, and the availability of a suitable substrate.[18] Specifically, the strong B−N bonds lead to the susceptibility of parasitic reactions between BCl_3 and NH_3.[19] Amano has introduced pulse-mode growth techniques, enhancing the surface migration of adhering atoms and consequently reducing parasitic gas-phase reactions.[20] Furthermore, experimentally determined high growth temperatures have been identified as a prerequisite for achieving single-phase h-BN, as evidenced by the successful synthesis of high-quality bulk h-BN at elevated temperatures of around 1500 °C.[21] Despite the large lattice mismatch between h-BN and sapphire substrates, sapphire substrates are commonly used as industrial-grade large-scale wafers in semiconductor materials. Therefore, producing large h-BN films on sapphire substrates remains necessary. Currently, there is little research on the preparation of h-BN films using HVPE, and the growth mechanism is not yet well-established, leaving ample room for significant improvement in crystal quality. In 2013, Coudurier et al. used high-temperature HVPE to grow a 2 μm-thick BN layer on an AlN/sapphire template at 1600 °C,[22] and the BN film exhibited a disordered turbostratic phase, with a c-lattice parameter of 6.78 Å, much greater than the value of the single-crystal h-BN.[12] Our group has also conducted preliminary investigations into the HVPE growth of h-BN micron films. The experimental results revealed that under low-pressure and high-temperature conditions, the crystalline quality of h-BN reaches its optimal level at a V/III ratio of 6.[23] In addition to the V/III ratio, the growth temperature significantly influences the surface migration of precursors, which in turn affects the morphology and crystal quality of h-BN.

In this study, low-pressure and high-temperature HVPE was used to grow h-BN micrometer films on *c*-plane sapphire substrates, with BCl_3 and NH_3 as the precursor gases. The influence of growth temperature on the surface morphology and crystal quality of h-BN was investigated. The microstructural characteristics of triangular grains on the surface of the h-BN film were comprehensively studied by transmission electron microscopy (TEM).

EXPERIMENTAL SECTION

A homemade high-temperature HVPE apparatus was used to grow h-BN, which could be heated to 1650 °C via induction heating. N_2, employed as a dilution and carrier gas, had a flow rate of 1 slm (standard liter per minute). BCl_3 and NH_3 were used as boron and nitrogen sources, respectively. To facilitate the surface migration of adatoms and diminish parasitic gas-phase reactions, NH_3 pulses were introduced.[24] A single NH_3 pulse cycle lasts for 60 s, with NH_3 flowing for the first 20 s, followed by no NH_3 input for the subsequent 40 s. In contrast, BCl_3 was continuously introduced throughout the entire growth process. The substrate was a 2 in. *c*-plane sapphire wafer, which was placed on a graphite susceptor. All samples maintained the same pressure (<100 Pa) and V/III ratio (6), with the only difference being the growth temperature (ranging from 1050 to 1650 °C).

The morphology of the h-BN films was measured by scanning electron microscopy (SEM) (TESCAN MAIA3 XMU). The crystallinity of the h-BN films was characterized by X-ray diffraction (XRD) (Bruker D8 ADVANCE). Raman spectroscopy (LabRAM ARAMIS) was introduced to measure the vibrational mode of B−N bonds in the h-BN films. The microstructure of h-BN grains was analyzed by TEM (JEM-2100Plus).

RESULTS AND DISCUSSION

We first investigate the influence of growth temperature on the morphology of BN by SEM. As depicted in Figure 1, the surface of the BN film grown at 1050 °C is covered with nanograins that are approximately 100 nm in size. As the growth temperature increases, these nanograins coalesce into smooth triangular grains. At 1450 °C, the triangular grains reach their maximum size of about 1 μm, indicating that lateral development occurs more frequently under this condition due

https://doi.org/10.1021/acs.cgd.3c01247
Cryst. Growth Des. 2024, 24, 810−816

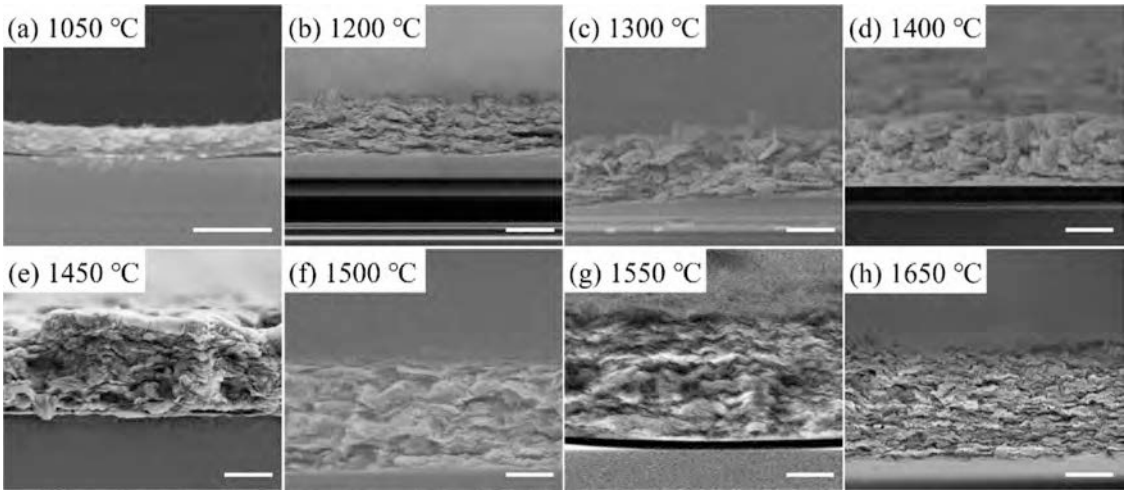

Figure 2. Cross-sectional SEM images of h-BN films grown at different temperatures. (a) 1050 °C. (b) 1200 °C. (c) 1300 °C. (d) 1400 °C. (e) 1450 °C. (f) 1500 °C. (g) 1550 °C. (h) 1650 °C. The scale bar is 500 nm.

to the enhanced surface migration of precursors.[17] However, as the growth temperature is further increased, both the size and density of the triangular grains decreased, eventually disappearing at 1650 °C, as illustrated in Figure 1f–h. Subsequent sections will provide an in-depth understanding of the crystallinity and orientation of these triangular grains. The aforementioned results reveal that by enhancing the growth temperature, BN exhibits a tendency to transition from a 3D growth to a 2D growth mode. However, solely manipulating the growth temperature is not sufficient to achieve complete 2D continuous growth of BN. We are currently attempting to adjust other growth parameters, such as the V/III ratio, pressure, carrier gas, etc., in order to obtain a smooth and continuous BN film. Additionally, cross-sectional SEM images (Figure 2) demonstrate that the BN films are stacked in layers and the growth rate (Figure S1) of BN increases with rising temperature. Nevertheless, the layer of h-BN appears rough, possibly attributed to the presence of turbostratic BN (t-BN) and amorphous BN (a-BN).[25] Furthermore, the wrinkling deformation of the BN layers may be caused by internal compressive stress and the loss of interlayer covalent bonds in the BN film.[26] Notably, the BN film has detached from the sapphire substrate, possibly due to stress introduced during the postgrowth cooling process.

XRD is used to assess the crystallinity of the BN films. As illustrated in Figure 3, XRD 2-theta scan patterns of all samples exclusively exhibit diffraction peaks corresponding to h-BN (0002) (26.7°) and (0004) (55°) diffraction peaks along with a sapphire (0006) diffraction peak at 41.8°.

This result indicates that the synthesized film is primarily oriented along the [0002] direction of h-BN, with an epitaxial relationship of $[0002]_{\text{h-BN}}/[0002]_{\text{sapphire}}$. As illustrated in Figure 4a, the (0002) diffraction peak of the h-BN film grown at 1050 °C appears broad and weak, suggesting either poor crystal quality or a very thin film. As the temperature rises, the h-BN (0002) diffraction peak becomes narrower. Notably, a distinct h-BN (0004) diffraction peak becomes visible at 1450 °C, indicating an enhancement in the crystal quality of h-BN relative to lower temperatures.

Raman spectroscopy is utilized to investigate the vibrational modes of the h-BN lattice resulting from bond stretching between boron and nitrogen atoms. As shown in Figure 4, Raman peaks of all h-BN samples are located in the range of

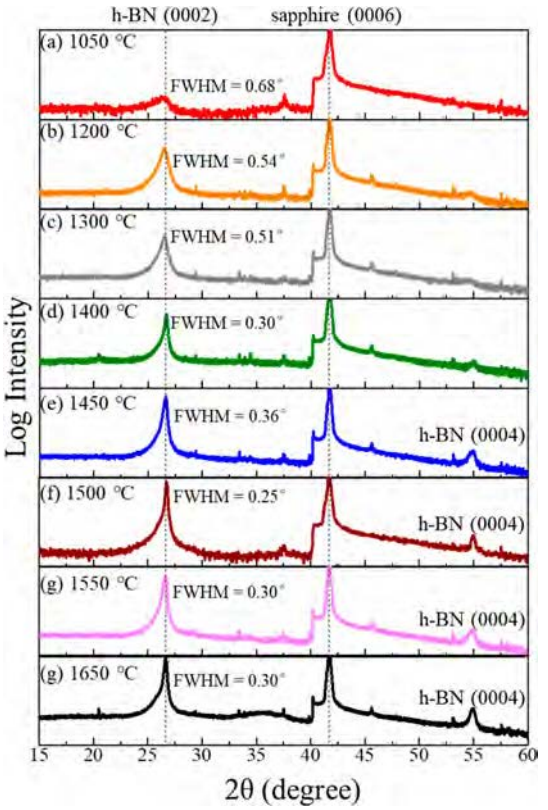

Figure 3. XRD 2θ scanning of h-BN films grown at different temperatures. (a) 1050 °C. (b) 1200 °C. (c) 1300 °C. (d) 1400 °C. (e) 1450 °C. (f) 1500 °C. (g) 1550 °C. (h) 1650 °C.

1368–1370 cm^{-1}, which corresponds to the E_{2g} vibrational mode of h-BN. Compared to the stress-free state, where the E_{2g} vibration peak is 1366 cm^{-1},[27] the E_{2g} peak of the h-BN film shifts to a higher phonon frequency. This shift is likely induced by compressive stress arising from the cooling process after growth.[28] The fwhm of each sample falls within the range of 20–50 cm^{-1}, indicating the presence of the t-BN phase or nanocrystals within the h-BN films.[29]

A systematic investigation of the orientation and crystallinity of triangular grains on the surface of h-BN is conducted using TEM. TEM samples are prepared from h-BN films grown at

https://doi.org/10.1021/acs.cgd.3c01247
Cryst. Growth Des. 2024, 24, 810–816

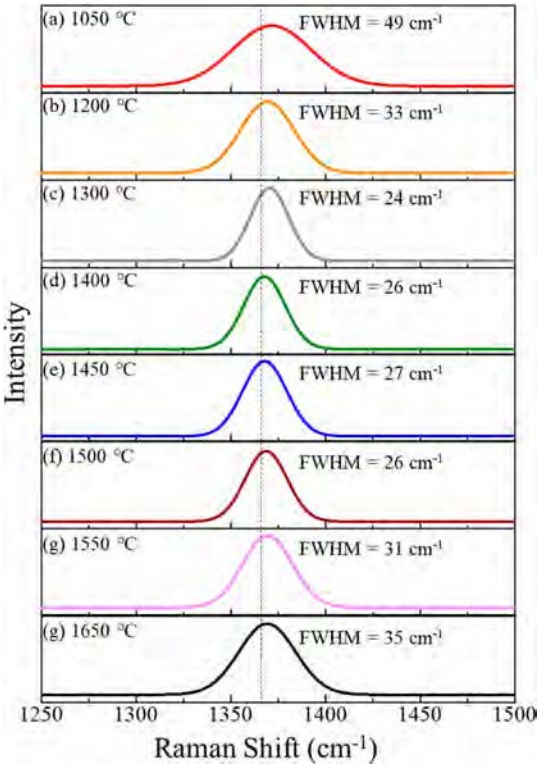

Figure 4. Raman spectra of h-BN films grown at different temperatures. (a) 1050 °C. (b) 1200 °C. (c) 1300 °C. (d) 1400 °C. (e) 1450 °C. (f) 1500 °C. (g) 1550 °C. (h) 1650 °C.

1450 °C, as shown in Figure 5a. Specifically, TEM samples are obtained by sectioning along the white dashed line using a focused ion beam (FIB), which intersects several triangular grains. As evident from the cross-sectional TEM image in Figure 5b, the cross sections of triangle grains marked by I, II, III, IV, and V exhibit an inverted triangle shape with a depth of approximately 1 μm. It is worth noting that the inverted triangular grains do not directly nucleate on the sapphire substrate but appear after a certain period of h-BN growth. Selected area electron diffraction (SAED) is utilized to ascertain the epitaxial relationship between the h-BN film and the sapphire substrate. The SAED pattern is taken from the h-BN/sapphire interface, where the incident azimuth is $[10\bar{1}0]_{sapphire}$. As illustrated in Figure 5c,d, the sapphire substrate diffraction spots conform to the $[10\bar{1}0]$ zone-axis diffraction pattern, whereas the h-BN film diffraction spots exhibit a ringlike pattern, indicating the presence of the t-BN and a-BN phase within the film. In Figure 5d, the most prominent diffraction ring corresponds to h-BN (0002), suggesting that the h-BN film is composed of a multitude of rotated and twisted subgrains oriented along the [0002] direction. In the (0002) diffraction ring, the spots in the vertical direction are brighter than in any other direction, indicating that the majority of h-BN subgrains have a [0002] orientation along the vertical direction, which parallels the [0002] direction of sapphire. Consequently, the epitaxial relationship between h-BN and sapphire is $[0002]_{h\text{-}BN}/[0002]_{sapphire}$, consistent with the XRD data in Figure 3. Furthermore, in the high-resolution TEM (HRTEM) image (Figure 5e), a 5 nm-thick amorphous layer separates the h-BN

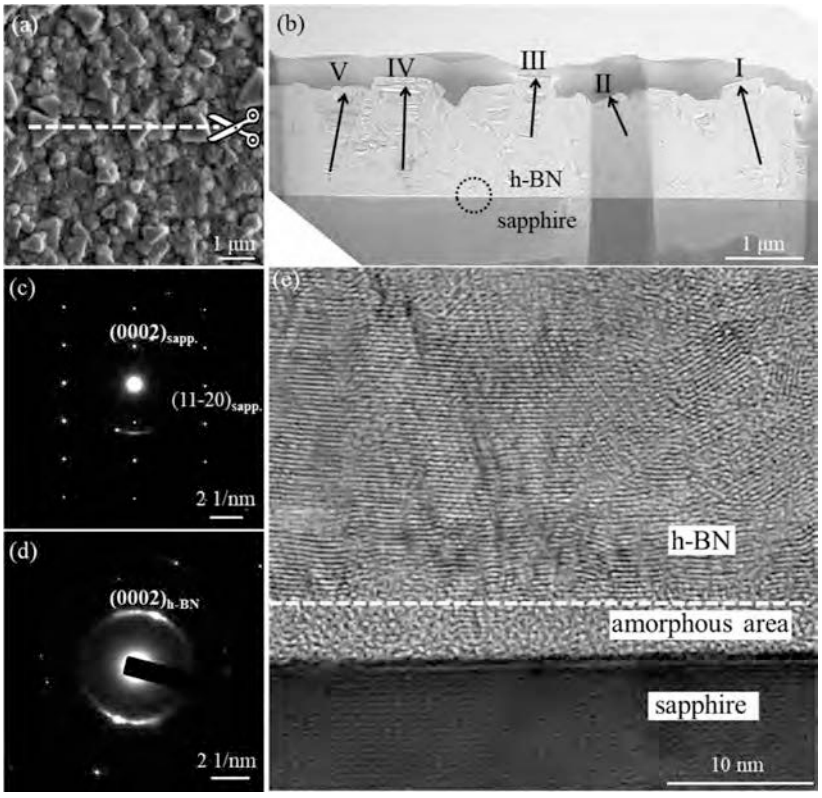

Figure 5. TEM characterization of the h-BN film grown at 1450 °C. (a) Surface SEM image of the h-BN film grown at 1450 °C, where the cutting line goes through several triangle grains. (b) Cross-sectional TEM image of the h-BN film in (a) and arrows representing the [0002] direction of the h-BN grain. (c) SAED pattern taken from the black circle in (b). (d) SAED pattern taken from the h-BN film. (e) HRTEM image taken from the black circle in (b).

https://doi.org/10.1021/acs.cgd.3c01247
Cryst. Growth Des. 2024, 24, 810−816

film from the sapphire substrate. This layer must have formed after the initial h-BN deposition, as the upper h-BN layer exhibits a well-defined epitaxial relationship with the underlying sapphire substrate.[30] The formation of this amorphous layer is likely related to the decomposition of the sapphire substrate at high temperatures.[31] Additionally, the (0002) lattice of h-BN is ordered during the initial stages of growth but becomes disordered after deposition exceeds 10 nm. This phenomenon arises since h-BN, being a vdW material, lacks out-of-plane chemical bonds, thereby weakening the epitaxial relationship between adjacent layers and making it difficult to achieve thick single-crystal h-BN films.

The internal structure of triangular grains is characterized using SAED and HRTEM. As shown in Figures 6a and S2,

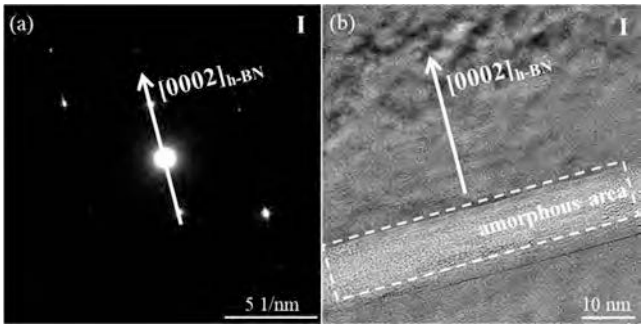

Figure 6. TEM analysis of triangle grains in the h-BN film. (a,b) Corresponding to SAED patterns and HRTEM images of triangle grain I in Figure 5b.

while these triangular grains do not exhibit complete 2D electron diffraction patterns, diffraction spots along the h-BN [0002] direction are discernible, indicating the growth of these triangular grains along the [0002] direction. Furthermore, the [0002] orientations of these grains are not entirely identical with a maximum deviation of 30°. Apart from the diffraction spots along the [0002] direction, diffraction spots in other directions are weaker or even absent, likely due to the curvature of the h-BN film disrupting the 2D lattice symmetry. HRTEM images in Figures 6b and S2 show that the (0002) crystal faces of these triangular grains are highly ordered, indicating excellent crystallinity. Notably, in the HRTEM image of grain I (Figure 6b), the region within the dashed lines appeared amorphous, possibly a result of weak interlayer forces leading to layering within the film. Although the interiors of these triangular grains are single-crystal h-BN, their bottoms are disordered and polycrystalline, as shown in Figure S3. Currently, the transformation of the film from a polycrystalline phase to single-crystal h-BN is not well-understood. If these single-crystal triangular grains with [0002] orientation could further expand laterally and coalesce into a continuous film, it might be possible to obtain thick single-crystal h-BN films. Further research is needed to explore how to suppress the generation of t-BN and a-BN phases, promote the coalescence of h-BN grains, and thus achieve high-quality thick single-crystal h-BN films. We believe that the key to obtain a continuous h-BN film is to promptly induce the transition of h-BN growth from a 3D mode to a 2D mode. To expedite this transition, it is essential to further increase the migration rate of B atoms and reduce parasitic reactions between B and N sources. Therefore, next, we will try to utilize a growth interruption method or flow modulation epitaxy,[26,32] where B and N sources are alternately introduced into the reactor. This will further enhance adatom surface migration and reduce parasitic gas-phase reactions, potentially allowing for the growth of larger-sized h-BN single-crystal thick films.

CONCLUSIONS

In conclusion, (0002) h-BN micrometer films are prepared on *c*-plane sapphire using low-pressure and high-temperature HVPE. The synthesized films exhibit a predominant orientation along the [0002] direction of h-BN and a typical layered cross-sectional morphology. As the growth temperature rises, h-BN nanograins on the surface coalesce into smooth triangular grains, and their dimension reaches micrometers at 1450 °C. These triangular grains are well-crystallized [0002]-oriented h-BN single crystals, as confirmed by SAED and HRTEM. The triangular grains are not formed directly from the sapphire substrate but rather appear during the process of growth. If these triangular grains could expand laterally and merge into films, it is anticipated that thick single-crystal h-BN films will be produced with large dimensions.

ASSOCIATED CONTENT

Supporting Information

The Supporting Information is available free of charge at https://pubs.acs.org/doi/10.1021/acs.cgd.3c01247.

Additional information including the deposition rate of the h-BN film as a function of growth temperature and TEM analysis of triangle grains in the h-BN film (PDF)

AUTHOR INFORMATION

Corresponding Authors

Shuxin Tan − *School of Electronics and Information, Nantong University, Nantong 226019, China*; Email: tansx2014@ntu.edu.cn

Jicai Zhang − *College of Mathematics and Physics, Beijing University of Chemical Technology, Beijing 100029, China; State Key Laboratory of Chemical Resource Engineering, Beijing University of Chemical Technology, Beijing 100029, China*; orcid.org/0000-0003-4945-6714; Email: jczhang@mail.buct.edu.cn

Authors

Ting Liu − *College of Mathematics and Physics, Beijing University of Chemical Technology, Beijing 100029, China*; orcid.org/0000-0001-7200-4009

Zhijie Shen − *College of Mathematics and Physics, Beijing University of Chemical Technology, Beijing 100029, China*

Minghao Chen − *College of Mathematics and Physics, Beijing University of Chemical Technology, Beijing 100029, China*

Qian Zhang − *College of Mathematics and Physics, Beijing University of Chemical Technology, Beijing 100029, China*

Maosong Sun − *College of Mathematics and Physics, Beijing University of Chemical Technology, Beijing 100029, China*

Chunlei Fang − *College of Mathematics and Physics, Beijing University of Chemical Technology, Beijing 100029, China*

Yong Lu − *College of Mathematics and Physics, Beijing University of Chemical Technology, Beijing 100029, China*

Hai Hu − *CAS Key Laboratory of Nanophotonic Materials and Devices, CAS Key Laboratory of Standardization and Measurement for Nanotechnology, CAS Center for Excellence in Nanoscience, National Center for Nanoscience and Technology, Beijing 100190, China*

https://doi.org/10.1021/acs.cgd.3c01247
Cryst. Growth Des. 2024, 24, 810−816

Complete contact information is available at:
https://pubs.acs.org/10.1021/acs.cgd.3c01247

Author Contributions

[⊥]T.L. and Z.S. authors contributed equally.

Notes

The authors declare no competing financial interest.

■ ACKNOWLEDGMENTS

This work was supported by the National Natural Science Foundation of China no. 52102152, no. 62074087, and no. 61874007, the Fundamental Research Funds for the Central Universities no. buctrc202127, Shandong Provincial Major Scientific and Technological Innovation Project no. 2019JZZY010209, and Key-Area Research and Development Program of Guangdong Province no. 2020B010172001.

■ REFERENCES

(1) Schué, L.; Sponza, L.; Plaud, A.; Bensalah, H.; Watanabe, K.; Taniguchi, T.; Ducastelle, F.; Loiseau, A.; Barjon, J. Bright Luminescence from Indirect and Strongly Bound Excitons in h-BN. *Phys. Rev. Lett.* **2019**, *122* (6), 067401.

(2) (a) Li, Y.; Lin, Z.; Zheng, W.; Huang, F. Micron-Thick Hexagonal Boron Nitride Crystalline Film for Vacuum Ultraviolet Photodetection with Improved Sensitivity and Spectral Response. *ACS Appl. Electron. Mater.* **2021**, *3* (9), 3774−3780. (b) Izyumskaya, N.; Demchenko, D. O.; Das, S.; Özgür, Ü.; Avrutin, V.; Morkoç, H. Recent development of boron nitride towards electronic applications. *Adv. Electron. Mater.* **2017**, *3* (5), 1600485.

(3) (a) Chen, Y.; Zou, J.; Campbell, S. J.; Le Caer, G. Boron nitride nanotubes: Pronounced resistance to oxidation. *Appl. Phys. Lett.* **2004**, *84* (13), 2430−2432. (b) Li, L. H.; Cervenka, J.; Watanabe, K.; Taniguchi, T.; Chen, Y. Strong Oxidation Resistance of Atomically Thin Boron Nitride Nanosheets. *ACS Nano* **2014**, *8* (2), 1457−1462. (c) Chen, X.; Tan, C. B.; Luan, K. R.; Wang, S.; Li, F. Y.; Liu, X. H.; Zhao, J. H.; Gao, Y. J.; Chen, Z. G. Epitaxially Grown Hexagonal Boron Nitride Films on Sapphire and Silicon Substrates. *Key Engineering Materials*; Trans Tech Publ., 2020; Vol. *843*, pp 90−96.

(4) Hod, O. Graphite and Hexagonal Boron-Nitride Possess the Same Interlayer Distance. *J. Chem. Theory Comput.* **2012**, *8*, 1360.

(5) Dean, C. R.; Young, A. F.; Meric, I.; Lee, C.; Wang, L.; Sorgenfrei, S.; Watanabe, K.; Taniguchi, T.; Kim, P.; Shepard, K. L.; Hone, J. Boron Nitride Substrates for High-Quality Graphene Electronics. *Nat. Nanotechnol.* **2010**, *5* (10), 722−726.

(6) Maity, A.; Grenadier, S.; Li, J.; Lin, J.; Jiang, H. X. Hexagonal Boron Nitride Neutron Detectors with High Detection Efficiencies. *J. Appl. Phys.* **2018**, *123* (4), 044501.

(7) Wang, M.; Meng, F.; Hou, D.; Han, Y.; Ren, J.; Bai, C.; Wang, B.; Zhou, T. Electronic Structure and Spin Properties Study on 2D h-BN Nanosheet with Ti or Fe Doping. *Solid State Commun.* **2020**, *307*, 113803.

(8) Naumov, I.; Bratkovsky, A. M.; Ranjan, V. Unusual Flexoelectric Effect in Two-Dimensional Noncentrosymmetric s p 2-Bonded Crystals. *Phys. Rev. Lett.* **2009**, *102* (21), 217601.

(9) (a) Watanabe, K.; Taniguchi, T.; Kanda, H. Direct-Bandgap Properties and Evidence for Ultraviolet Lasing of Hexagonal Boron Nitride Single Crystal. *Nat. Mater.* **2004**, *3* (6), 404−409. (b) Kubota, Y.; Watanabe, K.; Tsuda, O.; Taniguchi, T. Deep Ultraviolet Light-Emitting Hexagonal Boron Nitride Synthesized at Atmospheric Pressure. *Science* **2007**, *317* (5840), 932−934.

(10) Wang, G.; Meng, J.; Chen, J.; Cheng, Y.; Huang, J.; Zhang, S.; Yin, Z.; Jiang, J.; Wu, J.; Zhang, X. W. Epitaxy of Hexagonal Boron Nitride Thin Films on Sapphire for Optoelectronics. *Cryst. Growth Des.* **2022**, *22* (12), 7207−7214.

(11) (a) Liu, S.; He, R.; Xue, L.; Li, J.; Liu, B.; Edgar, J. H. Single Crystal Growth of Millimeter-Sized Monoisotopic Hexagonal Boron Nitride. *Chem. Mater.* **2018**, *30* (18), 6222−6225. (b) Shi, Z.; Wang, X.; Li, Q.; Yang, P.; Lu, G.; Jiang, R.; Wang, H.; Zhang, C.; Cong, C.; Liu, Z.; Wu, T. R.; Wang, H. M.; Yu, Q. K.; Xie, X. M. Vapor-Liquid-Solid Growth of Large-Area Multilayer Hexagonal Boron Nitride on Dielectric Substrates. *Nat. Commun.* **2020**, *11* (1), 849.

(12) Kobayashi, Y.; Akasaka, T. Hexagonal BN epitaxial Growth on (0 0 0 1) Sapphire Substrate by MOVPE. *J. Cryst. Growth* **2008**, *310* (23), 5044−5047.

(13) Pierucci, D.; Zribi, J.; Henck, H.; Chaste, J.; Silly, M. G.; Bertran, F.; Le Fevre, P.; Gil, B.; Summerfield, A.; Beton, P. H.; Novikov, S. V.; Cassabois, G.; Rault, J. E.; Ouerghi, A. Van der Waals Epitaxy of Two-Dimensional Single-Layer h-BN on Graphite by Molecular Beam Epitaxy: Electronic Properties and Band Structure. *Appl. Phys. Lett.* **2018**, *112* (25), 253102.

(14) Chen, J.; Wang, G.; Meng, J.; Cheng, Y.; Yin, Z.; Tian, Y.; Huang, J.; Zhang, S.; Wu, J.; Zhang, X. W. Low-Temperature Direct Growth of Few-Layer Hexagonal Boron Nitride on Catalyst-Free Sapphire Substrates. *ACS Appl. Mater. Interfaces* **2022**, *14* (5), 7004−7011.

(15) Wang, G.; Huang, J.; Zhang, S.; Meng, J.; Chen, J.; Shi, Y.; Jiang, J.; Li, J.; Cheng, Y.; Zeng, L. B.; Yin, Z. G.; Zhang, X. W. Wafer-Scale Single Crystal Hexagonal Boron Nitride Layers Grown by Submicron-Spacing Vapor Deposition. *Small* **2023**, *19*, 2301086.

(16) (a) Gong, X.; Xu, K.; Huang, J.; Liu, T.; Ren, G.; Wang, J.; Zhang, J. Evolution of the Surface Morphology of AlN Epitaxial Film by HVPE. *J. Cryst. Growth* **2015**, *409*, 100−104. (b) Fujito, K.; Kubo, S.; Nagaoka, H.; Mochizuki, T.; Namita, H.; Nagao, S. Bulk GaN Crystals Grown by HVPE. *J. Cryst. Growth* **2009**, *311* (10), 3011−3014.

(17) Umehara, N.; Masuda, A.; Shimizu, T.; Kuwahara, I.; Kouno, T.; Kominami, H.; Hara, K. Influences of Growth Parameters on the Film Formation of Hexagonal Boron Nitride Thin Films Grown on Sapphire Substrates by Low-Pressure Chemical Vapor Deposition. *Jpn. J. Appl. Phys.* **2016**, *55* (5S), 05FD09.

(18) Kobayashi, Y.; Akasaka, T.; Makimoto, T. Hexagonal Boron Nitride Grown by MOVPE. *J. Cryst. Growth* **2008**, *310* (23), 5048−5052.

(19) Coudurier, N.; Chubarov, M.; Boichot, R.; Mercier, F.; Blanquet, E.; Reboud, R.; Lay, S.; Crisci, A.; Coindeau, S.; Encinas, T.; et al. Growth of boron nitride films on w-AlN (0001), 4° off-cut 4H-SiC (0001), W (110) and Cr (110) substrates by Chemical Vapor Deposition. *Cryst. Res. Technol.* **2016**, *51* (3), 231−238.

(20) Yang, X.; Nitta, S.; Nagamatsu, K.; Bae, S.-Y.; Lee, H.-J.; Liu, Y.; Pristovsek, M.; Honda, Y.; Amano, H. Growth of Hexagonal Boron Nitride on Sapphire Substrate by Pulsed-Mode Metalorganic Vapor Phase Epitaxy. *J. Cryst. Growth* **2018**, *482*, 1−8.

(21) Watanabe, K.; Taniguchi, T.; Kanda, H. Direct-Bandgap Properties and Evidence for Ultraviolet Lasing of Hexagonal Boron Nitride Single Crystal. *Nat. Mater.* **2004**, *3* (6), 404−409.

(22) Coudurier, N.; Boichot, R.; Mercier, F.; Reboud, R.; Lay, S.; Blanquet, E.; Pons, M. Growth of Boron Nitride on (0001) AlN Templates by High Temperature-Hydride Vapor Phase Epitaxy (HT-HVPE). *Physics Procedia* **2013**, *46*, 102−106.

(23) Liu, T.; Li, X.; Zhao, J.; Zhang, Q.; Lu, Y.; Xu, J.; Tan, S.; Zhang, J. C. Hexagonal Boron Nitride Film on Sapphire Substrate Grown by Low-Pressure and High-Temperature Halide Vapor Phase Epitaxy. *J. Cryst. Growth* **2022**, *588*, 126655.

(24) Yang, X.; Nitta, S.; Nagamatsu, K.; Bae, S.-Y.; Lee, H.-J.; Liu, Y.; Pristovsek, M.; Honda, Y.; Amano, H. Growth of Hexagonal Boron Nitride on Sapphire Substrate by Pulsed-Mode Metalorganic Vapor Phase Epitaxy. *J. Cryst. Growth* **2018**, *482*, 1−8.

(25) Guo, Q.; Xie, Y.; Yi, C.; Zhu, L.; Gao, P. Synthesis of Ultraviolet Luminescent Turbostratic Boron Nitride Powders via a Novel Low-Temperature, Low-Cost, and High-Yield Chemical Route. *J. Solid State Chem.* **2005**, *178* (6), 1925−1928.

(26) Chugh, D.; Wong-Leung, J.; Li, L.; Lysevych, M.; Tan, H. H.; Jagadish, C. Flow Modulation Epitaxy of Hexagonal Boron Nitride. *2D Mater.* **2018**, *5* (4), 045018.

(27) Saha, S.; Rice, A.; Ghosh, A.; Hasan, S.; You, W.; Ma, T.; Hunter, A.; Bissell, L.; Bedford, R.; Crawford, M.; et al.

Comprehensive Characterization and Analysis of Hexagonal Boron Nitride on Sapphire. *AIP Adv.* **2021**, *11* (5), 055008.
(28) Chen, X.; Tan, C.; Liu, X.; Luan, K.; Guan, Y.; Liu, X.; Zhao, J.; Hou, L.; Gao, Y.; Chen, Z. Growth of Hexagonal Boron Nitride Films on Silicon Substrates by Low-Pressure Chemical Vapor Deposition. *J. Mater. Sci.: Mater. Electron.* **2021**, *32* (3), 3713−3719.
(29) Ahmed, K.; Dahal, R.; Weltz, A.; Lu, J.-Q.; Danon, Y.; Bhat, I. Growth of Hexagonal Boron Nitride on (111) Si for Deep UV Photonics and Thermal Neutron Detection. *Appl. Phys. Lett.* **2016**, *109* (11), 113501.
(30) Snure, M.; Paduano, Q.; Kiefer, A. Effect of Surface Nitridation on the Epitaxial Growth of Few-Layer sp2 BN. *J. Cryst. Growth* **2016**, *436*, 16−22.
(31) Yang, X.; Nitta, S.; Pristovsek, M.; Liu, Y.; Nagamatsu, K.; Kushimoto, M.; Honda, Y.; Amano, H. Interface Amorphization in Hexagonal Boron Nitride Films on Sapphire Substrate Grown by Metalorganic Vapor Phase Epitaxy. *Appl. Phys. Express* **2018**, *11* (5), 051002.
(32) Zhang, Q.; Guo, Y.; Liu, Z.; Wang, D.; Li, Q.; Yan, J.; Li, J.; Wang, J. Effect of the Growth Interruption on the Surface Morphology and Crystalline Quality of MOCVD-Grown h-BN. *Crystals* **2023**, *13* (3), 486.

https://doi.org/10.1021/acs.cgd.3c01247
Cryst. Growth Des. 2024, 24, 810−816